ASI

Carbon – Science and Technology

ISSN 0974 – 0546

http://www.applied-science-innovations.com

ARTICLE Received: 08/05/2016, Accepted: 24/07/2016

Facile one-spot synthesis of highly porous KOH-activated carbon from rice husk: Response surface methodology approach

Tran Van Thuan [(A)], Van Thi Thanh Ho [(B)], Nguyen Duy Trinh [(A)], Nguyen Thi Thuong [(A)], Bui Thi Phuong Quynh [(A)], and Long Giang Bach [(A, *)]

(A) NTT Institute of High Technology, Nguyen Tat Thanh University, 300A Nguyen Tat Thanh Str., Ward 13, District 4, Ho Chi Minh City, Vietnam.
(B) Hochiminh City University of Natural Resources and Environment, 236B Le Van Sy Str., Ward 1, Tan Binh District, Ho Chi Minh City, Vietnam.
*Corresponding Author, E-mail address: blgiangntt@gmail.com

Abstract: Highly porous *KOH*–activated carbon was successfully synthesized from rice husk by chemical activation with KOH. The products were characterized by IR, SEM, and BET. The response surface methodology (RSM) was employed to determine the optimum fabrication conditions of AC with respect to the simultaneous effects of activation temperature (*T*), impregnation rate (*IR*) and activation time (*t*) to maximize the yield of activated carbon and removal efficiency of Ni^{2+}. The optimum synthesis conditions were T = 522 ^{o}C, IR = 1.3 and t = 360 min with a maximum AC yield of 28.5 % and a maximum Ni^{2+} removal of 28.5 %. The results indicated that highly porous structure, high surface area as well as the surface functional groups are key impacts in the adsorptive capacity of activated carbons for Ni^{2+}.

Keywords: Adsorption of Ni (II), rice husk, response surface methodology, activated carbon.

1. Introduction: Groundwater contamination by nickel is considered as one of the environmentally serious issues because of its toxicological influences on human health [1-3]. The presence of nickel metal in micro–organisms can be a culprit of vulnerable diseases such as vomiting, chest pain, and rapid respiration. According to the World Health Organization (WHO), the critical concentration of nickel in drinking water is 0.02 ppm [4]. Several strategies have been proposed to remove the Ni^{2+} ions from aqueous solutions including ion exchange, chemical precipitation, ultrafiltration, electrochemical deposition, and adsorption [5 - 11]. Activated carbon (AC) has been extensively used in adsorption technique. It can effectively capture the heavy metal ions owing to many potential properties such as high porosity and a variety of functional groups [12-14]. However, commercial AC is very expensive, and hence its potential applications are prohibited by some economical obstacles. To overcome this drawback, the fabrication of AC from abundant agricultural by–products is considered as an effective choice.

Rice husk is normally treated as waste at fields after manufacturing of rice products in some tropical countries, causing serious environmental problems. Therefore, it is necessary to make full use of this widespread and zero-cost source. Various reports have been

investigated such as the employment of rice husk as biomass source to produce biofuel or the use of rice husk as precursors to produce concrete, zeolite, AC and silica [15-19]. Notably, not only do the processing and transformation of rice husk to AC solve the environment problems, but also provided the high-quality products with porous structure, high surface area and low–cost for water and wastewater treatment.

In our study, we used the KOH as an eco–friendly and favorable activating agent to inhibit tar formation and to develop the porous structure via chemical activation in high temperature. Moreover, significant effects of fabrication conditions involving activation temperature, impregnation rate and activation time on formation yield of AC and removal percentage of Ni^{2+} were assessed by surface response plots from mathematical tool RSM for the optimization process. Moreover, the analysis of variance (ANOVA) and coefficients of regression (R^2) were used to assess the fitness of the obtained models and the significance of influential variables [20, 21].

2. Experimental

2.1. Chemicals and instruments: All chemicals for this study were commercially purchased from Merck and used as received without any further purification unless otherwise noted. The scanning electron microscope (SEM) was recorded by instrument S4800, Japan and used an accelerating voltage source of 10 kV with a magnification of 7000. The FTIR spectra were recorded by using the Nicolet 6700 spectrophotometer instrument. The N_2 adsorption/desorption isotherm was obtained using the Micromeritics 2020 volumetric adsorption analyzer system and BET surface area was calculated using the Brunauer–Emmet–Teller (BET) equation.

2.2. Production of AC: The dried rice husk was first pyrolyzed at 500 ^oC (10 ^oC/min) for 1 h under nitrogen atmosphere. The resulting char was then soaked with KOH solution for 24h. IR between KOH and the char was calculated as follows:

$$IR = \frac{w_{ZnCl_2}}{w_{Precursor}}$$

where, w_{KOH} and w_{char} are the weight of the anhydrous KOH (g) and the char (g), respectively.

The *KOH*–impregnated char samples were heated under nitrogen at various *T* for different *t*. Finally, the receiving *KOH*–AC was repeatedly washed with deionized water and dried at 105 ^oC. The formation yields of AC were calculated as follows:

$$AC\ yield\ (\%) = \frac{w_{AC}}{w_o}.100 \quad (2)$$

where, w_{AC} and w_O are the weight of AC (g) and dried weight of precursor (g), respectively.

2.3. Adsorption batch: The activated carbons (0.25 g) were poured into an Erlenmeyer flask containing 50 mL of aqueous solution of Ni^{2+} 50 ppm. The mixture was agitated until obtaining absorption equilibrium. The AC was then removed from the mixture using filter paper. The residual Ni^{2+} concentrations were determined by AAS and the percentage of Ni^{2+} removal was calculated by the following equation:

$$Ni^{2+}removal(\%) = \frac{C_o - C_e}{C_o}.100 \quad (3)$$

where, C_o and C_e are initial and equilibrium Ni^{2+} concentrations (ppm), respectively.

2.4. Experimental design with RSM: RSM technique is used to optimize experimental results through second order polynomial regression equations, which describe the true mathematical relationship between the response (*y*) and the set of independent values (*x*) by two–order polynomial equations. Central composite design (CCD) is used to establish given 20 experiments (Table 1). Accordingly, five level was investigated including the low (encoded –1), high (encoded +1) and rotatable

(encoded ±α). Analysis of variance (ANOVA) is calculated using Design–Expert version 9.0.5.1 (DX9).

Table 1 Independent variables matrix and their encoded levels

No	Independent factors	Code	Levels				
			–α	-1	0	+1	+α
1	T (^{o}C)	x_1	332	400	500	600	668
2	IR (-)	x_2	0.16	0.5	1.0	1.5	1.84
3	t (min)	x_3	9.5	30	60	90	110.5

3. Results and discussion

3.1. Assessment of experimental results with Design-Expert: The experimental and predicted results of AC yield and Ni^{2+} removal efficiency were presented in Table (2). The value range of the actual variables was designed as follows: T from 332 ^{o}C to 668 ^{o}C, IR from 0.16 to 1.84 and t from 9.5 min to 110.5 min. The correlation between the responses and variables was described by the following quadratic equations:

$$AC\,yield\,(\%) = 25.4 + 2.84x_1 + 3.97x_2 + 0.91x_3 - 2.68x_1x_2 - 0.35x_1x_3 - 0.1x_2x_3 + 0.31x_1^2 - 2.09x_2^2 - 0.91x_3^2$$

$$(4)\ Pb^{2+}\,removal\,(\%) = 97.8 + 2.67x_1 + 1.71x_2 - 0.81x_3 - 3.08x_1x_2 + 1.05x_1x_3 + 1.10x_2x_3 - 2.91x_1^2 - 0.79x_2^2 + 0.32x_3^2 \quad (5)$$

Table 3 showed the results of the ANOVA for response surface quadratic models. The significance of regression models can be assessed by R^2 and values of P. In detail, the P–values < 0.0001 and respective R^2 closer 1.0 indicate the proposed models are statistically significant at 95 % confidence level. Moreover, the high fitness of models was also confirmed by the adequate precision (AP) ratios, which both values were greater than 4.0 and by plots of predicted values versus actual values, which almost points positioned to the straight line (Figure 1). Besides, lack of fit (LOF) values was statistically insignificant and indicated the model fitted data well **[22]**.

Table 2 Matrix of observed and predicted values.

No	Variables			Actual (%)		Predicted (%)	
	x_1	x_2	x_3	AC yield	Ni^{2+} removal	AC yield	Ni^{2+} removal
1	400	0.5	30	12.2	90.0	11.9	90.0
2	600	0.5	30	24.3	98.8	23.6	99.0
3	400	1.5	30	25.3	96.5	25.4	96.9
4	600	1.5	30	28.0	95.2	26.4	95.1
5	400	0.5	90	14.7	84.8	14.6	86.0
6	600	0.5	90	26.7	97.0	24.9	97.7
7	400	1.5	90	28.7	94.9	27.7	95.9
8	600	1.5	90	28.7	95.6	27.3	96.7
9	332	1.0	60	21.6	86.7	21.5	85.7
10	668	1.0	60	28.7	94.5	31.1	93.9
11	500	0.16	60	12.0	94.0	12.8	93.3
12	500	1.84	60	24.7	99.2	26.2	98.3
13	500	1.0	9.5	20.7	99.7	21.3	99.9
14	500	1.0	110.5	22.7	99.8	24.4	98.0
15	500	1.0	60	24.6	96.3	25.4	97.8
16	500	1.0	60	24.4	96.0	25.4	97.8
17	500	1.0	60	25.3	97.8	25.4	97.8
18	500	1.0	60	26.2	99.1	25.4	97.8
19	500	1.0	60	26.8	98.9	25.4	97.8
20	500	1.0	60	25.7	98.5	25.4	97.8

Table 3. ANOVA for response surface quadratic models.

Response	Source	Sum of squares	Degree of freedom	Mean square	F-value	Prob. > F	Comment
AC yield (%)	Model	469.30	9	52.14	20.71	< 0.0001 [s]	Mean = 23.6
	x_1	109.90	1	109.90	43.64	< 0.0001 [s]	CV =6.72
	x_2	214.78	1	214.78	85.29	< 0.0001 [s]	R^2 = 0.9491
	x_3	11.19	1	11.19	4.44	0.0612 [n]	$R^2_{(adj.)}$ = 0.032
	$x_1 x_2$	57.24	1	57.24	22.73	0.0008 [s]	AP = 17.088
	$x_1 x_3$	0.98	1	0.98	0.39	0.5467 [n]	
	$x_2 x_3$	0.080	1	0.080	0.032	0.8621 [n]	
	x_1^2	1.41	1	1.41	0.56	0.4711 [n]	
	x_2^2	63.01	1	63.01	25.02	0.0005 [s]	
	x_3^2	11.85	1	11.85	4.70	0.0553 [n]	
	Residuals	25.18	10	2.52			
	Lack of Fit	20.90	5	4.18	4.88	0.0533 [n]	
	Pure Error	4.28	5	0.86			
Ni^{2+} removal (%)	Model	309.54	9	34.39	17.67	< 0.0001 [s]	Mean = 95.66
	x_1	82.26	1	82.26	42.26	< 0.0001 [s]	CV = 1.46
	x_2	30.31	1	30.31	15.57	0.0027 [s]	R^2 = 0.9408
	x_3	4.72	1	4.72	2.43	0.1504 [n]	$R^2_{(adj.)}$ = 0.8876
	$x_1 x_2$	58.32	1	58.32	29.96	0.0003 [s]	AP = 14.416
	$x_1 x_3$	3.65	1	3.65	1.87	0.2012 [n]	
	$x_2 x_3$	4.21	1	4.21	2.16	0.1724 [n]	
	x_1^2	115.73	1	115.73	59.45	< 0.0001 [s]	
	x_2^2	7.32	1	7.32	3.76	0.0813 [n]	
	x_3^2	2.32	1	2.32	1.19	0.3006 [n]	
	Residuals	19.47	10	1.95			
	Lack of Fit	10.59	5	2.12	1.19	0.4253 [n]	
	Pure Error	8.87	5	1.77			

Note: [s] significant at $p < 0.05$ and [n] not significant at $p > 0.05$.

3.2. Effect of variables on the AC yield and Pb^{2+} removal: Referring to Table (3), the T (x_1) and IR (x_2) were found to be strong effects on the formation yield of AC and the percentage of Ni^{2+} removal. While, the t (x_3) showed the insignificant effect on both responses because *P*–values of x_3, x_1x_3 and x_2x_3 were statistically insignificant and hence, t was maintained at zero level (*IR* = 1.0).

According to three–dimensional response surface plots in Figures (2C), the yield of AC was generally dependent on a various kind of T and IR. At low values of IR, the AC yield would increase extremely by increasing T from 332 ^oC to 668 ^oC. However, at a higher amount of activation agent, T slightly influenced on the AC yield. The value range of maximum yield was obtained at around 668^oC and IR = 1.0. As reported studies, the structural formation of AC must occur at appropriate T (commonly more than 350 ^oC), and hence very low temperature can be unfavorable for the fabrication of AC [15, 23-25].

According to the observation in Figure (2), the Ni^{2+} removal efficiency strongly depended on the AC, which were fabricated at various T and t. In detail, the yield of AC was favorable at a higher value of IR (1.0–1.84), while optimum T was determined at zero level (500 ^oC). Increasing the percentage of Ni^{2+} removal by increasing *IR*–value for the production of AC can be explained due to chemical agent which plays a crucial role in the development of new pore and essential functional groups for absorption of transition metal ions like Ni^{2+} [22]. The predicted optimal conditions based experiment were further conducted to verify the suitability of the proposed models: *T* = 522 ^oC, *IR* = 1.3 and *t* = 60 min (Figure 2). Thereby, the tests for AC yield and Ni^{2+} removal were obtained at 28.5 % and 99.7 %, which are nearly closed to the predicted values of 27.4 % and 98.5 %, respectively. These results demonstrated the high compatibility of the proposed models with the experimental data.

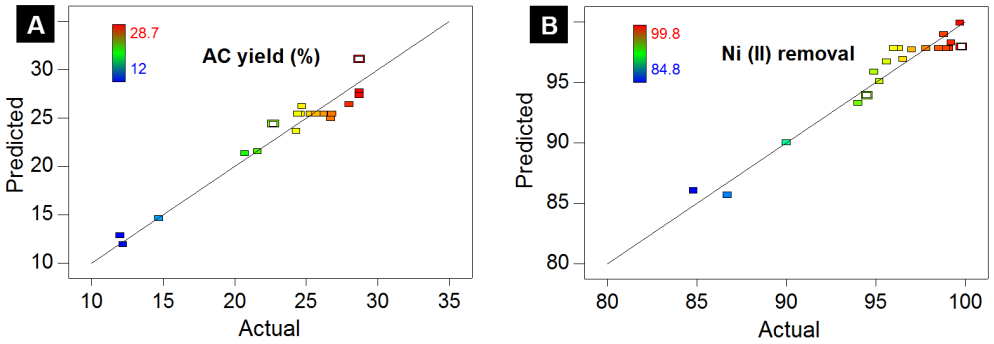

Figure (1): Actual versus predicted plot of regression models of AC yield (A) and Ni (II) removal (B).

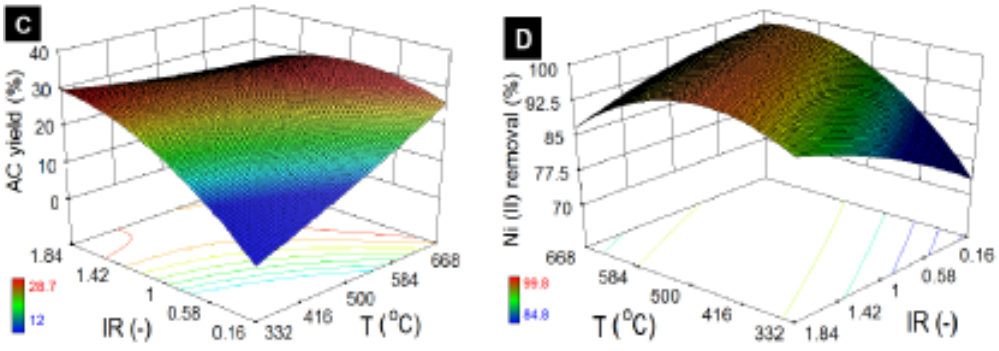

Figure (2): Effect of temperature T, IR and time t = 60 min on AC yield (C) and Ni^{2+} removal (D).

Table 4 Model confirmation

Sample	*T* (°C)	*IR* (-)	*t* (min)	Desirability	AC yield (%)		Ni^{2+} removal (%)	
					Predicted	Tested	Predicted	Tested
AC400	522	1.3	60	0.92	27.4	28.5	98.5	99.7

3.3. Characterization of synthesized AC: Figure (3) shows the FT-IR spectrum of the synthesized KOH–AC, which was generally found to possess various functional groups. In details, the presence of hydroxyl groups, O–H stretching and adsorbed water were confirmed by stretching vibration of broadband around 3400 cm^{-1} [26]. The shape peaks were positioned around 1680 cm^{-1} and 1545 cm^{-1} was attributed to the existence of the C=O group in the structure of aldehydes/ketones and O–N asymmetric stretch, respectively [27]. Moreover, the unsaturated bonds including C=C, C≡C could be recognized by the presence of shape peak at 1618 cm^{-1} and 2340 cm^{-1}, respectively.

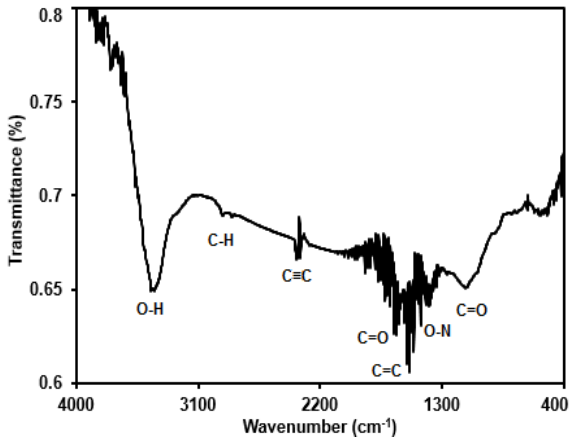

Figure (3). FT-IR spectra of the AC

Figure (4) shows SEM image the AC. It is obvious that the porous and defect structure of the as-syvnthesized AC was observed. This phenomenon can be explained due to the removal of non-carbon elements such as hydrogen, oxygen, and nitrogen released from the surface of char during pyrolysis process resulted in the formation of rigid carbon skeleton with rudimentary pore structure. Furthermore, the specific surface area for the AC sample obtained using the BET model was 253 m^2/g.

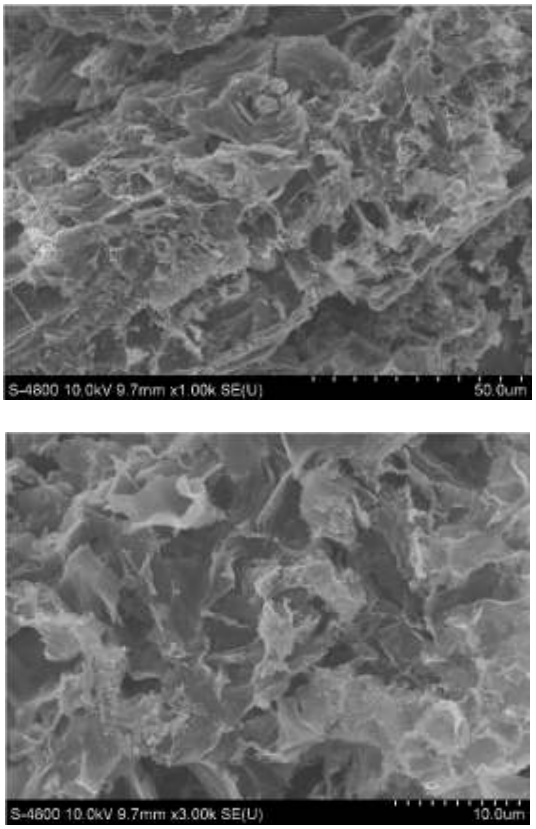

Figure (4). SEM image of the AC.

4. Conclusions: The highly porous rice husk–derived *KOH*–AC was successfully synthesized by chemical activation with KOH as the activating agent. By the use of the *RSM*–based quadratic regression equations, T and IR were found to cause strong effects on the AC yield and removal efficiency Ni^{2+}, while t was proved to be statistically insignificant. Alternatively, the maximum value of AC yield and Ni^{2+} removal was obtained 28.5 % and 99.7 %, respectively at predicted conditions: T = 522 °C, IR = *1.3* and t = 60 min. Based on these experimental results, we can demonstrate that a treatment process can be easily designed using rice husk for the fabrication of AC to remove toxic metal ions from the polluted water.

Acknowledgements
This research is funded by Foundation for Science and Technology Development Nguyen Tat Thanh University, Ho Chi Minh City, Vietnam.

Reference and notes

[1] V. K. Gupta, C. K. Jain, I. Ali, M. Sharma and V. K. Saini, Water Res. 37 (2003) 4038.
[2] M. I. Kandah and J. L. Meunier, J. Hazard. Mater. 146 (2007) 283.
[3] S. R. Popuri, Y. Vijaya, V. M. Boddu and K. Abburi, Bioresour. Technol. 100 (2009) 194.
[4] J. De Zuane, in Handbook of Drinking Water Quality, John Wiley & Sons, Inc. (2007) 49.
[5] B. Alyüz and S. Veli, J. Hazard. Mater., 167 (2009) 482.
[6] K. S. Hui, C. Y. H. Chao and S. C. Kot, J. Hazard. Mater. 127 (2005) 89.
[7] S. Mopoung, P. Amornsakchai, and S. Somroop, Carbon - Sci. Tech. 8 (2016) 1.
[8] A. S. Jadhav and G. T. Mohanraj Carbon – Sci. Tech. 8 (2016) 32.
[9] L. Giraldo, M. F. González-Navarro, Juan Carlos Moreno-Piraján, Carbon - Sci. Tech. 5 (2013) 303.
[10] S. Mopoung, S. Inkum, and L. Anuwetch, Carbon – Sci. Tech. 7 (2015) 24.
[11] C. Sumithra, S. C. Murugavel, and S. Karthikeyan, Carbon – Sci. Tech. 6 (2014) 342.
[12] K. Geetha, N. Velmani , S. Karthikeyan and P. S. Syed Shabudeen, Carbon – Sci. Tech. 6 (2014) 395.
[13] P. Shanthi, K. Jothi Venkatachalam, and S. Karthikeyan, Carbon – Sci. Tech. 6 (2014) 30.
[14] K. Anitha, P. S. Syed Shabudeen, S. Karthikeyan, and N.Aruna devi, Carbon – Sci. Tech. 7 (2015) 8.
[15] K. Le Van and T. T. Luong Thi, Prog. Nat. Sci. Mater. Int. 24 (2014) 191.
[16] H. T. Jang, Y. Park, Y. S. Ko, J. Y. Lee and B. Margandan, Int. J. Greenh. Gas Control 3 (2009) 545.
[17] W. Panpa and S. Jinawath, Appl. Catal. B Environ. 90 (2009) 389.
[18] G. Görhan and O. Şimşek, Constr. Build. Mater. 40 (2013) 390.
[19] A. Abbas and S. Ansumali, BioEnergy Res. 3 (2010) 328.
[20] S. Agarwal, I. Tyagi, V. K. Gupta, A. R. Bagheri, M. Ghaedi, A. Asfaram, S. Hajati, and A. A. Bazrafshan, J. Environ. Chem. Eng. 4 (2016), 1769.
[21] A. Tuna, A. Ozge, E. Ozdemir, E. B. Simsek, U. Beker, Water. Air. Soil Pollut. 224 (2013) 1685.
[22] U. K. Garg, M. P. Kaur, V. K. Garg and D. Sud, Bioresour. Technol. 99 (2008) 1325.
[23] N. Khan, E. M. Yahaya, M. Faizal, P. Mohamed and I. Abustan 11 (2010) 45.
[24] N. K. E. M. Yahaya, I. Abustan, M. Faizal, P. Mohamed, O. S. Bello, M. A. Ahmad and E. Campus, Int. J. Eng. Technol. 11 (2011) 186.
[25] N. K. E. M. Yahaya, M. Faizal, P. Mohamed, I. Abustan, O. S. Bello and M. A. Ahmad, Int. J. Eng. Technol. 10 (6) 47.
[26] N. K. E. M. Yahaya, M. F. M. L. Pakir, I. Abustan and M. A. Ahmad, Int. J. Eng. Technol. 10 (2010) 2.
[27] Y. Guo and D. A. Rockstraw, Microporous Mesoporous Mater. 100 (2007) 12.
[28] R. Sun and J. Tomkinson, Sep. Purif. Technol. 24 (2001) 529.

*****